In-situ forming supramolecular nanofiber hydrogel as a biodegradable liquid embolic agent for post-embolization tissue remodeling

Akihiro Nishiguchi[*1], Miho Ohta[1], Debabrata Palai[1], Shima Ito[1,2], Kensaku Mori[3], Ryotaro Akagi[4], Christophe Bajan[4], Guillaume Lambard[4], Keitaro Sodeyama[2,4], Tetsushi Taguchi*[*1,2]*

[1] Biomaterials Field, Research Center for Macromolecules and Biomaterials, National Institute for Materials Science, 1-1 Namiki, Tsukuba, Ibaraki 305-0044, Japan

[2] Faculty of Pure and Applied Sciences, University of Tsukuba, 1-1-1 Tennodai, Tsukuba, Ibaraki 305-8577, Japan

[3] Department of Radiology, Faculty of Medicine, University of Tsukuba, 1-1-1 Tennodai, Tsukuba, Ibaraki 305-8575, Japan

[4] Data-driven Materials Research Field, Center for Basic Research on Materials, National Institute for Materials Science, 1-1 Namiki, Tsukuba, Ibaraki 305-0044, Japan

E-mail: NISHIGUCHI.Akihiro@nims.go.jp, TAGUCHI.Tetsushi@nims.go.jp

Keywords: embolic agent • hydrogel • supramolecular chemistry • tissue remodeling • biopolymer

Embolic agents have been widely used to treat blood vessel abnormalities in interventional radiology as a minimally invasive procedure. However, only a few biodegradable liquid embolic agents exhibit high embolization performance, biodegradability, and operability. Herein, we report the design of in situ-forming supramolecular nanofiber (SNF) hydrogels as biodegradable liquid embolic agents with the assistance of Bayesian optimization through an active learning pipeline. Chemically modified gelatin with hydrogen-bonding moieties produced fibrin-inspired nanofiber-based hydrogels with a high blood coagulation capacity. The low viscosity of the SNF hydrogels made them injectable using a microcatheter, and the hydrogel showed sufficient tissue adhesion to the blood vessel walls and very weak adhesion to the catheter tubes. Moreover, the SNF hydrogels exhibited high blood compatibility, cytocompatibility, cell-adhesive properties, and biodegradability (in vitro and in vivo). Intravascularly delivered SNF hydrogels induced embolization of rat femoral arteries. This biodegradable liquid embolic agent could be a powerful tool for interventional radiology in the treatment of various diseases, including aortic aneurysm stent grafting, gynecological diseases, and liver cancer.

1. Introduction

Endovascular embolization in interventional radiology (IVR) is a minimally invasive procedure for the selective occlusion of diseased blood vessels, which reduces hospitalization time and the physical burden on patients.[1] Embolic agents are injected using a catheter guided by X-ray imaging and embolized at target sites to treat bleeding, cerebral aneurysms, malformations, uterine fibroids, and hepatocellular tumors.[2] These agents are categorized as solid and liquid types. Microparticle-based solid embolic agents composed of synthetic polymers, gelatin, and starch have been developed over the last decade owing to their biodegradability, imageability, and drug-loading ability.[3] However, solid embolic agents have some problems, including filling irregular target sites, cementing catheters, and proximal larger vessels by aggregation.[4]

Liquid embolic agents rapidly solidify blood after injection and can be applied to small and irregular target sites by tuning their viscosity.[5] However, conventional liquid embolic agents composed of synthetic polymers (e.g. poly(ethylene-co-vinyl alcohol) (EVOH), Onyx®) have drawbacks in incomplete aneurysm occlusion, recanalization, permanent neurological morbidity, and distal embolic events.[6] Moreover, cell infiltration and tissue remodeling do not occur because synthetic polymer-based embolic agents are non-biodegradable.[7] It has been reported that failure of regression of the aneurysm sac by tissue remodeling after an endovascular aneurysm leads to lower long-term survival.[8] Thus, tissue remodeling through cellular infiltration, vascularization, and biodegradation of embolic agents may be crucial for maintaining long-term occlusion and preventing recanalization. Although fibrin glue is a biodegradable liquid embolic agent, the typical occlusion time is a few minutes, and it may pass distally into other organs.[9] Further, some liquid embolic agents cause cementation of the catheter tube when injected. Although Onyx® was developed to avoid the issue observed in cyanoacrylate,[10] there are several drawbacks in irreversible adhesion to catheter tubes and recanalization postembolization, resulting in open surgical treatments and mortality in some cases.[11] Therefore, there is a need to develop liquid embolic agents that not only have high embolization performance but also biodegradability for tissue remodeling and operability. Although hydrogel-based liquid embolic agents, including temperature-responsive polymers,[12-13] shear thinning systems,[14-16] in situ crosslinking polymers,[17] and polymers with cationic and aromatic residues[18] have emerged as unique embolic agents, they have not been approved for endovascular embolization as they still need to fulfil the clinical requirements.

In a living system, hemostasis relies on a cascade of platelet activation and the formation of fibrin network structures. Fibrin fibers produced by crosslinking fibrinogen physically trap blood components such as blood cells, platelets, and other coagulation factors to form blood clots. Inspired by these biological systems, the use of nanofibrous materials as fibrin-mimicking hemostats for hemostasis has progressively increased.[19] Nanofibers possess a high surface area and fluid absorption capacity, which are advantageous for blood coagulation.[20] Although various nanofibrous materials such as peptide nanofibers[21] and electrospun nanofibers[22] have been used as hemostats, few examples of embolic agent applications have been reported. Endovascular injection of the peptide suspension may cause dilution under blood flow and pose a potential risk of distal embolization. Thus, ideally, a liquid embolic agent should be a solution before endovascular injection and should rapidly form in situ nanofiber network structures for embolization when injected.

Here, we describe the design of a supramolecular embolic agent that promotes tissue remodeling for IVR applications. Previously, we reported that an extracellular matrix-derived protein, gelatin (G), was modified with hydrogen-bonding moieties, ureidopyrimidinone units (UPy units), to obtain UPy-modified G (GUPy), which increased the mechanical strength of hydrogels through strong intermolecular hydrogen bonding.[23-25] We found that GUPy became water-insoluble by introducing a high degree of substitution (D.S.) of UPy units. This behavior was used to design a supramolecular biodegradable liquid embolic agent (Figure 1a). The high-D.S. GUPy is soluble in a mixture of dimethyl sulfoxide (DMSO) and ethanol and is injectable using a microcatheter. The injection of GUPy into the blood can produce a supramolecular nanofiber (SNF) hydrogel through solvent exchange and hydrogen-bonding-induced dimerization of UPy units, which can cause blood coagulation (Figure 1b). SNF hydrogels are biodegradable and cell-infiltrating, allowing tissue remodeling after embolization. We evaluated the viscosity, blood coagulation ability, injectability, adhesion to the blood vessel wall and catheter tube, and biodegradability of the SNF hydrogels, and embolization of the rat femoral artery. Moreover, machine-learning approaches were used to optimize embolic agents with lower viscosity and higher blood coagulation properties. This novel biopolymer-based embolic material may serve as an advanced liquid embolic agent to treat various diseases requiring material degradation and tissue remodeling, including aortic aneurysm stent grafting, gynecological diseases, and liver cancer.

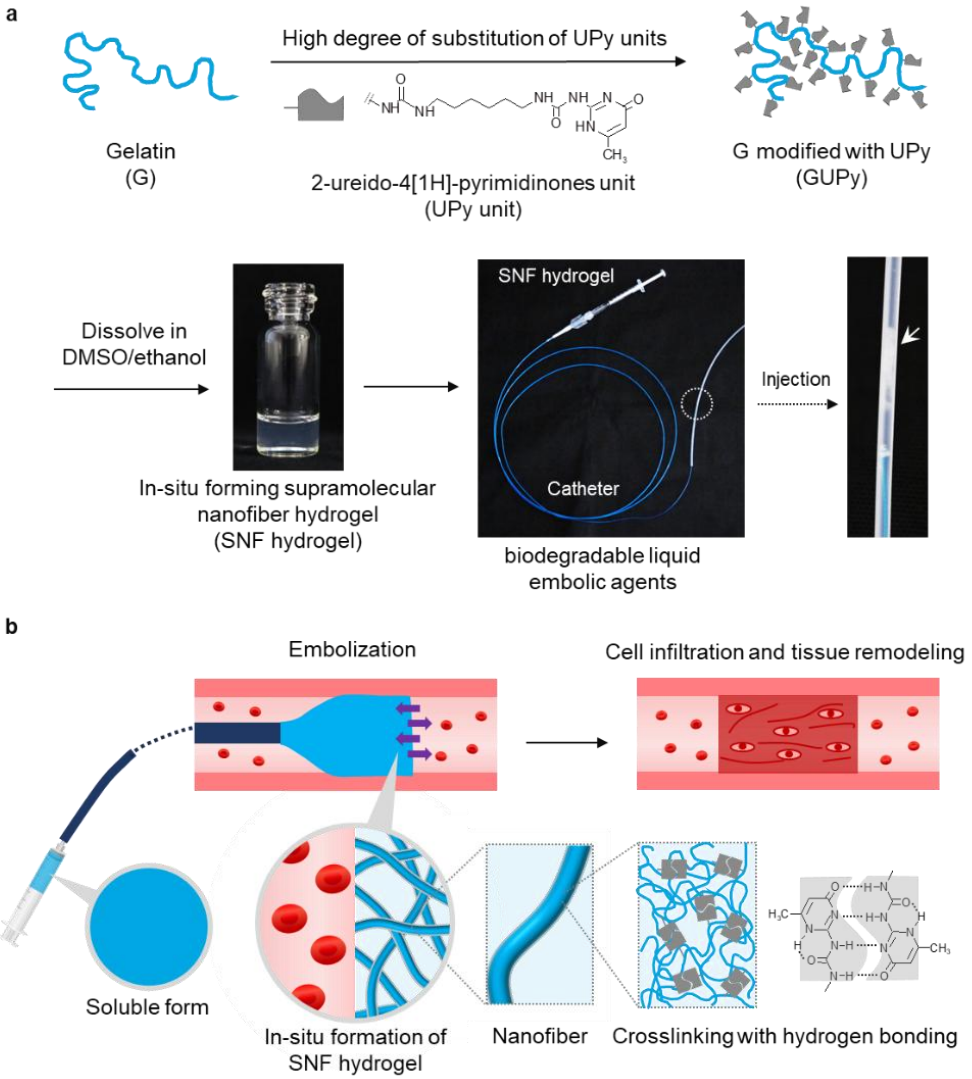

Figure 1. (a) Synthesis of gelatin modified with UPy units (GUPy) at high degree of substitution. and the preparation of in-situ forming supramolecular nanofiber (SNF) hydrogel for the embolization with a microcatheter. (b) Schematic illustration of the embolization process. Injected embolic agents can produce SNF hydrogel crosslinked with hydrogen bonding between UPy units in blood and support cell infiltration and tissue remodeling after the embolization.

2. Materials and Methods

2.1 Synthesis of GUPy

The synthesis of the UPy units has been reported in the literature.[26] GUPy was synthesized according to a previously reported method, with minor modifications.[23, 27] Porcine-derived gelatin (Nitta Gelatin Inc., Japan) were used for the modification with UPy units, tendon gelatin (tG, M_w = 344 kDa) and skin gelatin (sG(180), M_w = 180 kDa and sG(53), M_w = 53 kDa). tG or sG (1 g) was dissolved in DMSO (20 mL) at 50 ℃ under stirring. The UPy units (feed molar ratios: 2, 4, and 10) were dispersed in DMSO (5 mL) and added to the G solution. After stirring for 24 h at 25 ℃, the product was collected by precipitation with cold solvent mixture of ethanol and ethyl acetate (v/v=1/1). Precipitates were obtained by filtration through a glass filter and were washed with chloroform and ethanol. After vacuum drying for 2 days, GUPy derivatives with different feed molar ratios in a range of 2 to 10 (tGUPy-2, tGUPy-4, tGUPy-10, sG(180)UPy-4, sG(180)UPy-10, sG(53)UPy-4, sG(53)UPy-10) were obtained. The amino group content in TG was estimated using 2,4,6-trinitrobenzenesulfonic acid sodium salt dihydrate (Tokyo Chemical Industry Co., Ltd., Japan) according to a previous report.[28] The contents of UPy units in GUPy were measured using a microplate reader (Spark10M; TECAN, Switzerland). Each sample was dissolved in DMSO (0.25 mg/mL and added to a 96 well plate (film bottom). The absorbance was measured at 284 nm. 2(6-isocyanatohexylaminocarbonylamino)-6-methyl-4[1H]pyrimidinone was used as a standard, and the contents of UPy units were calculated using a standard curve.

2.2 Rheological measurement

GUPy was dissolved at 50 ℃ in DMSO under stirring, and ethanol was slowly added to the solution at 25 ℃. A viscometer (Viscomate; SEKONIC, Japan) was used to measure the viscosities of the embolic agents. To measure the shear modulus, GUPy solution (100 μL) was placed on the stage of rheometer (MCR301, Anton Paar GmbH, Austria) warmed at 37 ℃. A jig with a diameter of 10 mm was placed at a gap of 1 mm, and the solution was covered with saline (2 mL). The shear modulus was measured at 37 ℃ at a frequency of 10 rad/s with a 1% strain in an oscillatory mode. The values after 10 min were monitored and recorded.

2.3 Blood coagulation test

GUPy was dissolved in DMSO/ethanol and maintained at 37 ℃ until the use. Porcine blood (Tokyo Shibaura Zouki, Japan) was warmed at 37 ℃, and 100 μL of blood was mixed with 100 μL of GUPy solution by pipetting followed by vortexing for 5 s. After 3 min of incubation at

37 ℃, 1 mL of saline was added to wash non-gelling blood components, which were removed after centrifugation at 3000 rpm for 3 min. After repeating these steps three times, the blood aggregates were freeze-dried and weighed. The blood coagulation was calculated as:

$$\text{Blood coagulation (\%)} = W_m/(W_b + W_p) \quad (2)$$

where W_m, W_b, and W_d represent the dry weight of mixture of blood and polymer after washing and freeze drying, dry weight of blood, and dry weight of polymer, respectively.

The aggregates of tGUPy-4 and blood were observed by scanning electron microscopy (SEM, JCM-7000 NeoScopeTM, JEOL, Japan). Aggregates were fixed in paraformaldehyde and dehydrated using an ethanol/water gradient. *tert*-Butanol was added to the aggregates, which were then freeze-dried. The samples were then sputtered with platinum and observed at an accelerating voltage of 10 kV.

2.4 Fluorescence microscopy

Fluorescence-labeled tGUPy was used to observe the structure of embolic agents after gelation. tG (1 g) was dissolved in DMSO (20 mL) at 50 ℃ for 2 h. Fluoresceine isocyanate (1.1 mg, 2.9 μmol, 0.01 molar equivalent to amino groups in tG, Sigma-Aldrich, USA) was added to tG solution and stirred for 5 h. UPy unit (172 mg, 0.59 mmol, 4 molar equivalents to amino groups in tG) in DMSO (5 mL) was then added and stirred for 24 h at room temperature. After precipitation and washing in the same manner as for the synthesis of GUPy, the products were dissolved in 1 wt% phosphate-buffered saline (PBS, Nacalai Tesque, Inc., Japan) and dialyzed using a dialysis membrane (molecular weight cutoff: 10 kDa) for three days. After freeze-drying for three days, tGUPy-4-fluorescein was obtained. The products were dissolved in DMSO at 50 ℃ under stirring, and ethanol was slowly added to the solution at 25 ℃. PBS was added to a glass chamber slide, and the GUPy solution was slowly added to the PBS. The samples were observed using confocal laser scanning microscopy (CLSM, 900 with Airyscan2, Zeiss, Germany).

2.5 Swelling ratio

The 100 μL of tGUPy-4 solution was vortexed with 100 μL of saline for 10 s. The SNF hydrogels were collected after centrifugation for 5 s. After gelation at 37 ℃ for 1 h, PBS (pH = 7.4) was added to each tube and incubated for 24 h at 37 ℃, following which, the gels were collected and weighed (W_s). The swollen gels were desalted by incubation in water for 24 h, freeze dried, and weighed (W_d). The swelling ratio was calculated as:

$$\text{Swelling ratio} = (W_s - W_d)/W_d \quad (2)$$

where W_s and W_d represent the weight of swelled and dried gels, respectively.

2.6 Injectability test

The GUPy solution (1 mL, 4 wt%, DMSO:ethanol=7:3) was loaded into a 1 mL lock-type syringe. Syringes equipped with a 2.7 French (F) microcatheter (inner diameter 0.33 mm, Medtronic) were set to a compression-testing machine (EZ-LX, Shimadzu, Japan). Each syringe was subjected to increasing stress of up to 50 N at an approaching speed of 50 mm/min. The ejected gel was weighed, and the injectability was calculated as:

$$\text{Injectability (\%)} = W_e/W_o \times 100 \quad (3)$$

where W_o is the original weight of the adhesive before ejection, and W_e is the weight of the ejected hydrogel.

2.7 Tissue adhesion test

The adhesion test was performed according to previous report[7] with some modifications. Porcine carotid artery (Tokyo Shibaura Zouki, Japan) was used as the artery model. The carotid artery was washed with PBS, and one side was capped with a lure fit. The artery was filled with citrated whole blood, and 100 μL of tGUPy solution was injected into the artery using 1 mL syringe equipped with a thin tip (BETHEL, Japan) for 15 min. After 4 h of incubation at room temperature, the arteries were connected to a chamber for burst pressure measurements. The Lure fitting was removed, and a force was applied to measure the shear modulus. The burst strength (maximum pressure) was measured by running a saline solution using a syringe pump at a flow rate of 2 mL/min at 37 ℃.

2.8 Adhesiveness to polyethylene (PE) tube

Polyethylene (PE) tube A (inner diameter: 2 mm; outer diameter: 3 mm; length: 13 cm) was capped with a lure fitting and filled with PBS. PE tube B (inner diameter: 0.5 mm, outer diameter: 1 mm, 13 cm in length) was equipped with a 24 G needle and filled with tGUPy samples. PE tube-B was inserted 9 cm into PE-tube-A, and 50 μL of EVOH (Sigma-Aldrich, USA) dissolved in DMSO (8 wt%) and tGUPy-4 solution (4 wt%, 30% ethanol in DMSO) was slowly injected into PBS each in two installments. After incubation for 1 h at room temperature, the tensile strength was measured using a tensile tester (EZ-S 500N, Shimadzu, Kyoto, Japan).

2.9 Hemolysis assay

Rabbit-derived defibrinated blood was centrifuged at 200 ×*g* for 10 min. Precipitated blood cells were collected using a pipette and diluted with saline to 5% (*v*/*v*). Ultrapure water was used instead of saline to prepare the positive control. The 100 μL samples (water, DMSO, DMSO with 30% ethanol, EVOH (8 wt%, in DMSO), tGUPy-4 (4 wt%, 30% ethanol in DMSO)) were mixed with 1 mL of the diluted suspension of blood cells. After the incubation at 37 ℃ for 4 h, the solution was centrifuged at 500 ×*g* for 5 min, and 100 μL of supernatant was transferred to a 96-well microplate. The absorbance was measured at 540 nm using a microplate reader, and the hemolysis percentage was calculated from the absorbance. The absorbance of water-treated samples was set to 100%. The hemolysis ratio was calculated as:

$$\text{Hemolysis ratio (\%)} = (A_s - A_p)/ (A_d - A_p) \times 100\% \quad (4)$$

where A_s, A_p, and A_d were the absorbance of samples, physiological saline, and DI water, respectively.

2.10 Cell culture

Normal human dermal fibroblasts (NHDFs, Lonza, USA) were cultured in RPMI1640 medium supplemented with 10% fetal bovine serum (Sigma-Aldrich, USA) and 1% penicillin-streptomycin (Thermo Fisher Scientific, USA). For the observation of cell adhesion onto gels, tGUPy-4 solution (100 μL, 4 wt%, DMSO:ethanol=7:3) and EVOH (100 μL, 8 wt%, in DMSO) was added to a cell culture insert (24 well, PET, 8-μm pore, Corning, USA). PBS was added to the plate, and the plate was incubated for 1 h for gelation. PBS (2 mL) was then added to the insert and plate, and the plate was incubated for 1 h. After washing gels with PBS three times, cells (1×10^4) were seeded into the gels and cultured for 24 h at 37 ℃ in a 5% CO_2 incubator. To evaluate cell proliferation, tGUPy solution (50 μL, 4 wt%, DMSO:ethanol=7:3) was injected to PBS in a 24-well plate to form gels after 5 min of incubation. After washing three times with PBS, the cells (2×10^4) were seeded onto the gels and cultured for 24 h. Cells were counted using a cell counting kit (WST-8 assay, DOJINDO, Japan). Briefly, 10 μL of WST-8 reagent was added to 100 μL of culture medium and incubated for 2 h. The absorbance of the medium was monitored at 450 nm using a microplate reader. The cell numbers were calculated using a standard curve.

2.11 Fluorescence staining

NHDFs were fixed with 4% paraformaldehyde for 1 h. After washing with PBS, cells were treated with 0.2% Triton-X for 30 min for permeabilization. Cells were blocked with 1% BSA/PBS for 1 h. For actin staining, cells were stained with rhodamine-labeled phalloidin (1:200, Thermo Fisher Scientific, USA) overnight at 4 ℃. After washing with PBS, the cells were observed by CLSM.

2.12 Degradation test with collagen

GUPy gels (500 μL, 4 wt%, DMSO:ethanol=7:3) were mixed with Tris-HCl buffer solution (0.1 M) with 5 mM $CaCl_2$ (0.5 mL, pH = 7.4) by vortexing. After centrifugation at 3000 rpm for 3 min, the supernatant was removed. The precipitates were washed with PBS (10 mL) for 5 min with shaking to remove the DMSO. After washing, the samples were treated with collagenase (0.1 mg/mL, 12 U/mL) in the buffer solution at 37 ℃ for 1, 3, 6, and 24 h. After the incubation, the supernatants were removed, and ultrapure water was added and incubated at 25 ℃ for 1 h for the desalination. The resulting gel was freeze-dried and weighed.

2.13 Subcutaneous implantation of embolic agents

All the animal experiments were approved by the Animal Care and Use Committee of the National Institute for Materials Science (No. 76-2023-19). tGUPy-4 was dissolved in DMSO containing 30% ethanol and filtrated using a 0.45-μm filter for the sterilization. The 100 μL of tGUPy-4 solution (4 wt%, 30% ethanol in DMSO) and EVOH (8 wt%, in DMSO) was mixed with 100 μL of saline and vortexed for 10 s. After centrifugation for 5 s, the hydrogels were collected and placed in a silicone mold (2 mm thickness). After 10 min, the hydrogels were transferred to a Petri dish filled with 20 mL saline solution and incubated for 30 min. After repeating the washing process three times, hydrogels were obtained. Mice (7-week-old female C57BL/6J, 20-25 g, Jackson Laboratory, USA) were anesthetized by inhalation of 2% isoflurane. Hair was shaved from the backs of mice, and the shaved areas were disinfected with 70% ethanol. The hydrogels were subcutaneously implanted into the backs of the mice. At 1, 3, 7, 14, and 28 days after implantation, the mice were euthanized by blood removal, and tissues were collected. The samples were then fixed in 10% formalin buffer solution for three days and sectioned. Images of the hematoxylin and eosin-stained tissues were scanned using a digital slide scanner (NanoZoomer S210, Hamamatsu Photonics, Hamamatsu, Japan).

2.14 Embolization of femoral artery

Rats (8-week-old male Sprague–Dawley, 250-300 g, Jackson Laboratory, USA) were anesthetized by inhalation of 2.5% isoflurane. Hair was shaved from the legs of mice, and the

right hindlimb was disinfected using 70% ethanol. After a skin incision, 100 μL of tGUPy-4 solution was injected into the femoral artery for embolization. The skin was closed using 3-0 suture. After disinfecting the incision, the rats were intraperitoneally administered carprofen (5 mg/kg) for analgesia and amikacin (1 mg/kg). The rats were then placed on a heating plate at 37 °C under anesthesia to measure blood perfusion. Blood perfusion of the normal (left) and ischemic limbs (right) was monitored using a laser Doppler imaging system (OZ-2Pro, OMEGAWAVE, Tokyo, Japan) pre-/post-treatment and at 1, 7, and 14 days. An average blood flow > 6 s was recorded.

2.15 Exploration of embolic agents using active learning

Active learning is a general framework which includes the "learning" step formed from past experiments and a set of actions resulting from the experimental feedback, the "active" step. Many learning-acting cycles form an active learning pipeline. In this study, we report using an active learning pipeline assisted by Bayesian optimization (ALBO) to optimize salient input features among three experimentally tunable process parameters for achieving low viscosity and high blood coagulation capacity in embolic agents.

First, we defined a fixed protocol for building our dataset composed of the embolic agent properties Ψ = {viscosity, blood coagulation capacity} and tunable process parameters θ = {UPy_ratio, Conc, EtOH_amount}, where UPy_ratio is the feeding ratio of UPy, Conc is the concentration, EtOH_amount is the ethanol amount. Each tunable process parameter $\theta_i \in \theta$ was restricted to vary within a domain d_i with a resolution δd_i, both chosen to be experimentally feasible, as summarized in Table 1.

Table 1. List of tunable process parameters θ i $\in$ θ, with their accessible domain di and resolution δ di chosen for the optimization of embolic agents.

Process parameter θ_i	Domain d_i	Resolution δd_i
UPy_ratio (%)	[100, 1000]	100
Conc (wt%)	[1, 8]	1
EtOH_amount (%)	[0, 4]	0.5

At this stage, 100 × 8 × 9 = 7,200 combinations of θ_i were experimentally possible. Then, a cycle of the ALBO pipeline, summarized in Fig. 6(a), is conducted as follows:

(i) A Gaussian process is trained on a set {θ, Ψ} of n samples, n=40 samples initially before using ALBO, that serves as a surrogate function S to exploit and explore θ;

(ii) A set θ* of 10 samples that maximize an acquisition function (here, the expected improvement) is proposed for experimental feedback. Steps (i) and (ii) represent the Bayesian optimization part in the ALBO pipeline here.
(iii) θ* is experimentally evaluated, and corresponding Ψ* properties are reported. If Ψ* are judged satisfactory enough, the ALBO pipeline is stopped; otherwise, another cycle (i)–(iii) is started by adding newly acquired experimental data to the set {θ, Ψ} of samples.

The MADGUI[29] system was employed to implement this ALBO pipeline for optimizing embolic agents with lower viscosity and higher blood coagulation properties. This approach allows for efficient exploration of the parameter space without intuiting the θ-to-Ψ relationship, which can be particularly challenging given the non-linear nature of the process-property relationships in complex materials like embolic agents.

2.16 Statistical analysis

The results are expressed as the mean ± SD. One-way analysis of variance (ANOVA), followed by Tukey's multiple comparison post hoc test, was used to test for differences among groups. Experiments were repeated multiple times as independent experiments. The data shown in each figure are complete datasets from representative independent experiments. None of the samples were excluded from the analysis. Statistical significance is indicated as $*P < 0.05$, $**P < 0.01$, and $****P < 0.0001$. Statistical analyses were performed using GraphPad Prism software (version 8.0; GraphPad Software).

3. Results and Discussion

3.1 Engineering biodegradable liquid embolic agents

To develop embolic agents with a low viscosity and high blood coagulation ability, properties such as solubility, viscosity, shear modulus, and blood coagulation were evaluated (Figure 2a). The effects of several parameters, including the feeding ratio of the UPy unit (2, 4, and 10 equivalents to amino groups in G), concentration of G (1, 2, 4, 6, and 8 wt.%), solvent type (DMSO/ethanol = 100/0, 80/20, and 70/30), and molecular weight of gelatin (M_w = 21, 53, 180, and 340 kDa), were investigated to explore embolic agents. Note that DMSO and ethanol are clinically used as solvents for embolic agents (e.g. Onyx®). The GUPy derivatives with different feed molar ratios in a range of 2 to 10 (tGUPy-2, tGUPy-4, tGUPy-10, sG(180)UPy-4, sG(180)UPy-10, sG(53)UPy-4, sG(53)UPy-10) are summarized in Table S1. The introduction of the UPy units into G was characterized using ^{1}H NMR spectroscopy (Figure S1). The benchmark of viscosity and blood coagulation were set to <30 mPa•s (e.g. Onyx32: 32 mPa•s) and >80%, respectively. EVOH solution dissolved in DMSO was used as a model of Onyx®. The ethanol concentration and content drastically affected the solubility of gelatin, with 16 of the 59 samples being insoluble (Figure 2b). When tGUPy derivatives (tGUPy-2, -4, and -10) were dissolved in DMSO at more than 4 wt%, the viscosity exceeded over 30 mPa•s. To decrease the viscosity, ethanol was added to gelatin solution. Ethanol, as a poor solvent for G, may cause partial aggregation of G and interfere with the interaction between G and DMSO, resulting in a decrease in viscosity. Although unmodified gelatin (G) formed a precipitate in DMSO/ethanol mixture solvents, GUPy derivatives were completely soluble in 30% ethanol solvent in DMSO. The viscosity of all tGUPy derivatives at 4 wt% were < 30 mPa•s, and tGUPy-4 decreased the viscosity from 75.7 mPa•s in DMSO to 28.6 mPa•s in 30% ethanol in DMSO (62% decrease).

To characterize the mechanical properties of the hydrogels, the shear moduli of the embolic agents after immersion in PBS were measured using a rheometer. Rheological measurements showed that the storage modulus (*G*') of tGUPy-4 was over 100 Pa and tGUPy-4 formed hydrogel-like precipitates, while original tG was dissolved in water (Figure 2c). The precipitates were in hydrogel form, and the swelling ratio of tGUPy-4 was 3.8 (Figure S2). tGUPy-2 showed lower *G*' than that of tGUPy-4 and tGUPy-10 due to lower D.S. of UPy units. These results indicated that hydrogen bonding between the UPy units induced precipitation. EVOH possessed over 35000 Pa modulus and formed non-hydrated solid-like precipitates. Blood coagulation was evaluated by mixing the blood with embolic agents. The tGUPy

derivatives showed high blood coagulation ability, whereas tG dissolved in the blood (Figure 2d). Some sG(180)UPy and sG(53)UPy showed blood coagulation ability, but their viscosities were relatively high. Although EVOH is known to possess blood coagulation ability, the values obtained in these experiments were relatively low because the coagulation speed was rapid, and EVOH did not mix well with blood. Taken together, tGUPy-2, -4, and -10 solution (4 wt%, 30% ethanol) possessed optimal properties to satisfy the required properties of viscosity (<30 mPa•s) and blood coagulation (>80%) (Figure 2e). In the following experiments, tGUPy-4 solution (4 wt%, 30% ethanol) was used as the embolic agent.

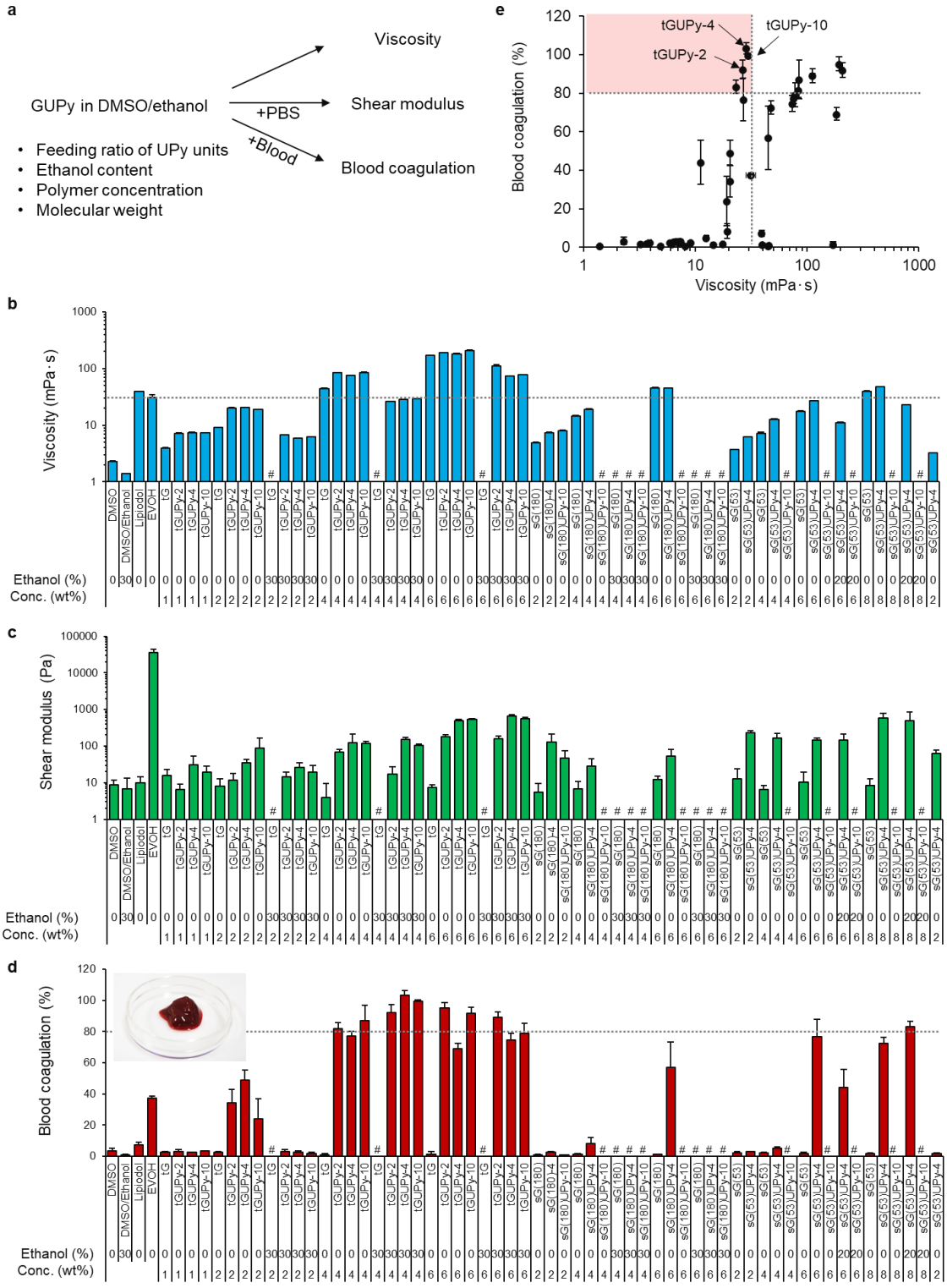

Figure 2. (a) Gelatin derivatives were dissolved in DMSO/ethanol mixture solvents and the viscosity, shear modulus, and blood coagulation were evaluated. (b) Viscosity, (c) shear modulus, and (d) blood coagulation of embolic agents with different parameters including feeding ratio of UPy unit, concentration of G, solvent composition (Ethanol/DMSO mixture), and molecular weight of gelatin (n = 3). # denotes that polymer did not dissolve in the solvents. (e) Relationship between viscosity and blood coagulation plotted from the result of Figure 2b and d. Conc. indicates concentration. Data are presented as the mean ± s.d..

3.2 Structural observation of SNF hydrogels

Engineered tGUPy solution (tGUPy-4, 4 wt%, 30% ethanol) formed hydrogels when injected into PBS, whereas tG solution dissolved in PBS (Figure 3a). Competitive inhibition of hydrogen bonding using urea (10 M) completely dissolved the hydrogels, indicating that the UPy units functioned as non-covalent crosslinking points to form hydrogels. CLSM observations of the hydrogels in PBS revealed that they possessed three-dimensional interconnected fibrous structures (Figure 3b). The fibrous network structures were three-dimensionally distributed (Figure 3c). These results indicate that the tGUPy solution transformed into nanofiber network structures in response to solvent exchange and sequential hydrogen bonding between the UPy units, which produced hydrogels composed of SNF hydrogels.

Scanning electron microscopy (SEM) revealed that the fiber diameter was approximately 270 nm, which was similar to the diameter of fibrin fibers (~200 nm) (Figure 3d,e).[30] Engineered nanofiber network structures are structurally analogous to fibrin networks, which play a central role in the blood coagulation cascade. Fibrous structures promote blood coagulation by physically trapping blood components and forming blood clots. When tGUPy was mixed with blood, the nanofiber networks were entangled with blood components such as red blood cells and formed dense aggregates, which may facilitate blood coagulation (Figure 3f). The blood coagulation kinetics were monitored using a rheometer (Figure 3g). *G'* of GUPy increased soon after mixing with blood, and hydrogels were formed. On the other hand, although the addition of only solvents to blood showed relatively high initial *G'* due to the formation of the aggregation, *G'* did not increase and no coagulation occurred. To enhance the contrast of the embolic agents for IVR, iohexol was added to the GUPy solution. Tantalum powder has been used as a contrast agent in Onyx®, but it cause image artifacts for angiography[31] and a tattoo-like staining on the skin surfaces.[32] Iohexol is water soluble, clinically used as intravascular contrast agent with 46.4% iodine by molecular weight. It has been reported that 30 wt.% iohexol can provide sufficient pixel intensity with adequate visibility.[16] Although the addition of iohexol slightly increased the viscosity and decreased blood coagulation, we confirmed that the GUPy solution with 30 wt% iohexol had a relatively low viscosity and showed high blood coagulation ability (Figure S3).

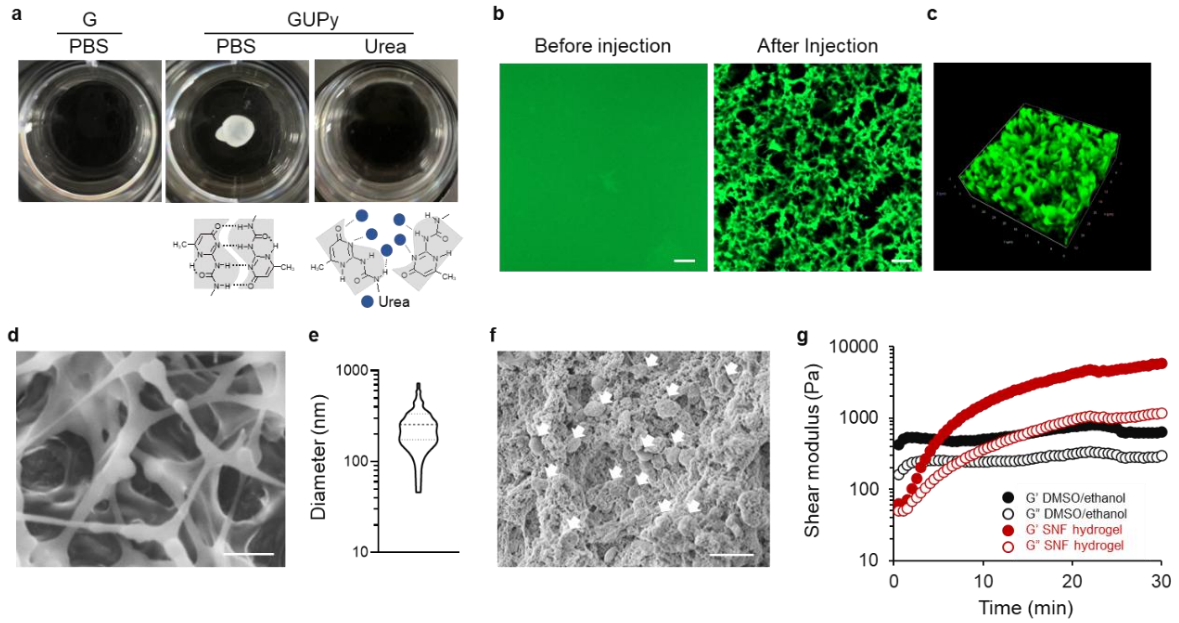

Figure 3. (a) Photos of tG and tGUPy-4 solution injected into PBS (37 ℃). For blocking test, GUPy solution was injected into urea solution (10 M). (b) Confocal laser scanning microscopy (CLSM) images of GUPy solution before and after the injection into PBS. Fluorescein-modified tGUPy-4 was used for the visualization. (c) Three-dimensional-reconstructed CLSM image of supramolecular nanofiber (SNF) hydrogel. (d,e) Scanning electron microscopy (SEM) image and distribution of fiber diameter in SNF hydrogels (80 fibers were counted). (f) SEM image of mixture of SNF hydrogel with blood. (g) Rheological measurements of SNF hydrogel when mixed with blood. Blood was added to GUPy solution on a stage of rheometer, and time-dependent shear modulus change was monitored. Data are presented as the mean ± s.d.. Scale bars represent 10 μm for (b,f) and 1 μm for (d).

3.3 Injectability and tissue-adhesive property

In situ-formed SNF hydrogels composed of GUPy solution were injected using a microcatheter (2.7 F) (Figure 4a). To evaluate injectability, the SNF hydrogels were injected into PBS using a microcatheter, and the force required for injection was measured (Figure 4b). The force was dependent on the polymer concentration and a 4 wt% solution was injected with an injection force of less than 20 N, which was the injectable range for the operator (Figure 4c).[33] The injectability of SNF hydrogels was over 90% (Figure 4d). These results suggest that the SNF hydrogels can be used as liquid embolic agents in microcatheter applications.

Next, we investigated the tissue adhesive properties of the SNF hydrogels using ex vivo artery models. The porcine-derived carotid artery was filled with citrated whole blood, and the hydrogel was injected using a needle to demonstrate G inside the carotid artery (Figure 4e). Cross-sectional observation of the H&E-stained tissues showed that the hydrogel adhered to the surface of the blood vessels (Figure 4f). SNF hydrogels showed almost same adhesion strength to carotid artery compared to that of EVOH as a model of Onyx® (Figure 4g). SNF hydrogels were initially low viscous when injected to the blood vessels and glued into the gap in the tissues. Then, it underwent phase transition from liquid to gel due to solvent exchange, resulting in tissue adhesion. These results indicate that SNF hydrogels possess embolic properties comparable to those of clinically available embolic agents.

Although embolic agents need to adhere to the blood vessel walls after injection, their adhesion to the catheter tube is not desirable because of the risk of hemorrhage during extraction and open surgery to remove the catheter.[34] To confirm the adhesive properties of the embolic agents to the catheter tubes, the adhesion strengths of the SNF hydrogel and EVOH to a polyethylene tube were measured (Figure 4h). The adhesion strength of the SNF hydrogel showed 10 times-fold decrease compared than that of the EVOH hydrogel partially due to the difference of the hydrophobicity (Figure 4i and j). This result indicates that the SNF hydrogels do not cause irreversible adhesion to the catheter tubes, and the catheter can be removed after treatment, which can prevent postoperative complications.

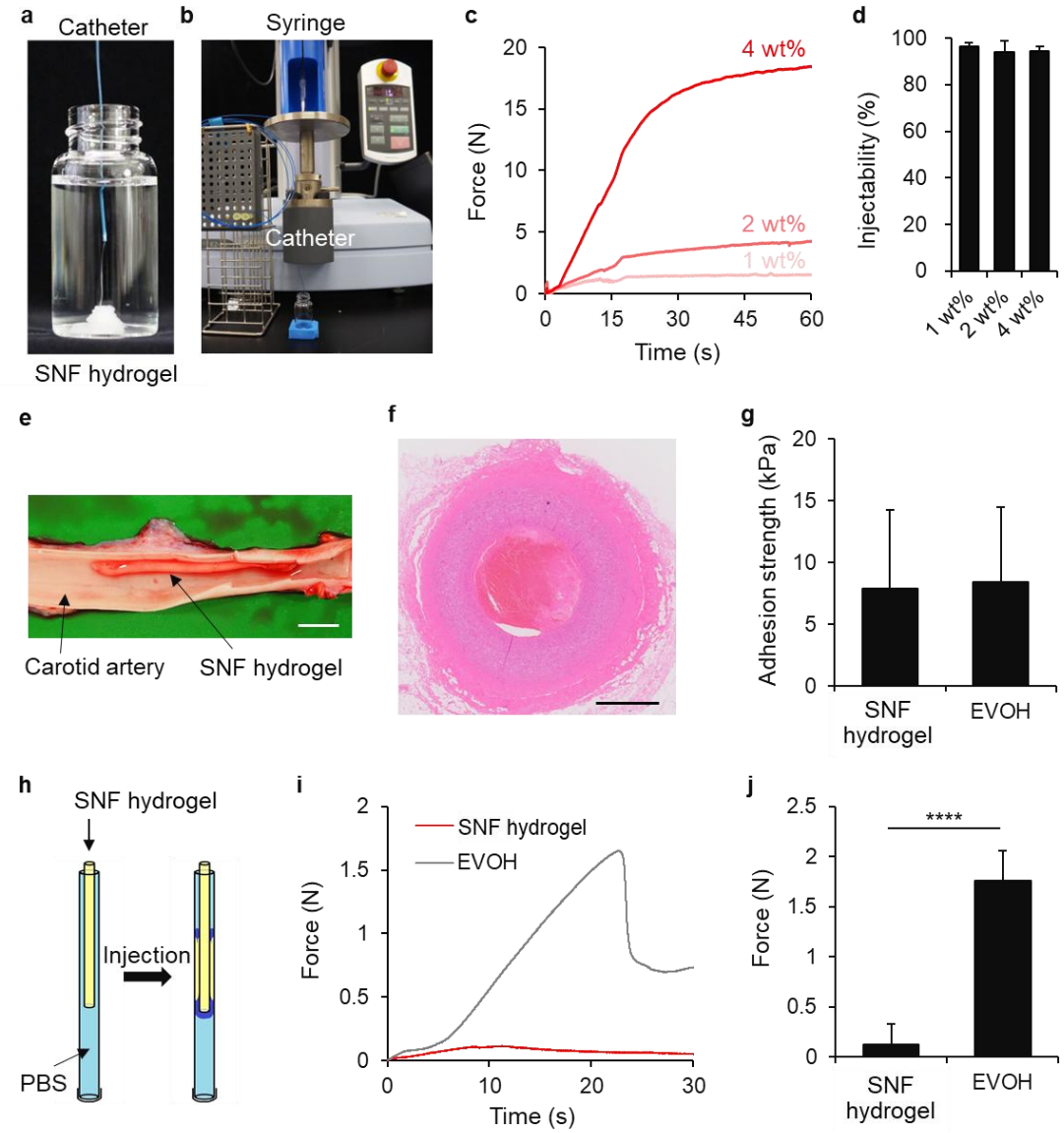

Figure 4. (a) Photo of injection of tGUPy solution using a microcatheter (2.7 F). (b) Setup of injectability test. (c,d) Force curves and injectability of tGUPy at 1, 2, and 4 wt% (n = 3). (e) Photo of tGUPy hydrogels injected into a lumen of carotid artery filled with citrated whole blood. (f) HE image of tGUPy hydrogels in carotid artery. (g) Adhesion strength of EVOH and tGUPy (n = 6). (h) Setup of adhesion test to PE tube. (i) Force curves of EVOH and tGUPy. (j) The maximum forces during 30 s of measurements (n = 4). Data are presented as the mean ± s.d. ****$P < 0.0001$ analyzed by Student's *t*-test. Scale bars represent 1 mm for (f) and 1 cm for (e).

3.4 Biodegradability of SNF hydrogels

To assess the hemocompatibility of the SNF hydrogels, a hemolysis assay was performed using defibrinated rabbit blood. Similar to EVOH, the SNF hydrogel did not cause hemolysis, indicating high hemocompatibility (Figure 5a). The cell-adhesive properties of the SNF hydrogels were evaluated by culturing human fibroblasts on the hydrogels. For post-embolization tissue remodeling, the hydrogels formed must be biocompatible, biodegradable, and cell-adhesive for cell infiltration. CLSM observations showed that NHDFs adhered and spread on the SNF hydrogels, whereas EVOH did not support cell adhesion (Figure 5b). Because SNF hydrogels are composed of an extracellular matrix-derived gelatin with cell-adhesive ligands (RGD sequences), they function as a suitable cell-adhesive scaffold. EVOH was not suitable for cell adhesion, partially because of the hydrophobic surfaces for cell adhesion and the instability of the precipitates. Moreover, the SNF hydrogels supported the proliferation of NHDFs during incubation (Figure 5c).

Subsequently, in vitro and in vivo biodegradability tests were performed. Treatment with collagenase enzymatically degraded the SNF hydrogels, which remained stable in the absence of collagenase (Figure 5d). Gelatin-based materials were degraded by enzymes secreted by infiltrating cells. For the in vivo biodegradability test, the SNF hydrogels were subcutaneously implanted into mice. Histological observations revealed that SNF hydrogels gradually degraded in vivo, and the cross-sectional area decreased to approximately 40% at 8 weeks after subcutaneous implantation, whereas synthetic polymer-based EVOH precipitates did not degrade (Figure 5e,f). F4/80 stained cross-sectional images showed that macrophages accumulated around SNF hydrogels, which might be associated with degradation of the hydrogels (Figure S4). Moreover, the SNF hydrogels were injected into the femoral arteries of rats to embolize them (Figure 5g). Laser Doppler imaging and histological observation showed that blood flow was inhibited by the injection of SNF hydrogels, and the severe necrosis in the legs was confirmed on day 14, indicating successful embolization of the femoral artery (Figure 5h,i).

Most clinically available liquid embolic agents are non-biodegradable, and it has been reported that chronic foreign body responses are confirmed after embolization using EVOH.[35] In the case of SNF hydrogels, many cells (e.g., immune cells and fibroblasts) infiltrated the hydrogels during degradation and fibrous tissues were newly formed, indicating that the tissue remodeling process was initiated in the hydrogels. Oklu et al. highlighted the importance of cell infiltration into embolic agents and tissue remodeling in the treatment of aneurysms.[16] Thus,

this gelatin-based liquid embolic agent could be valuable as a biodegradable liquid embolic agent that promotes tissue remodeling after embolization.

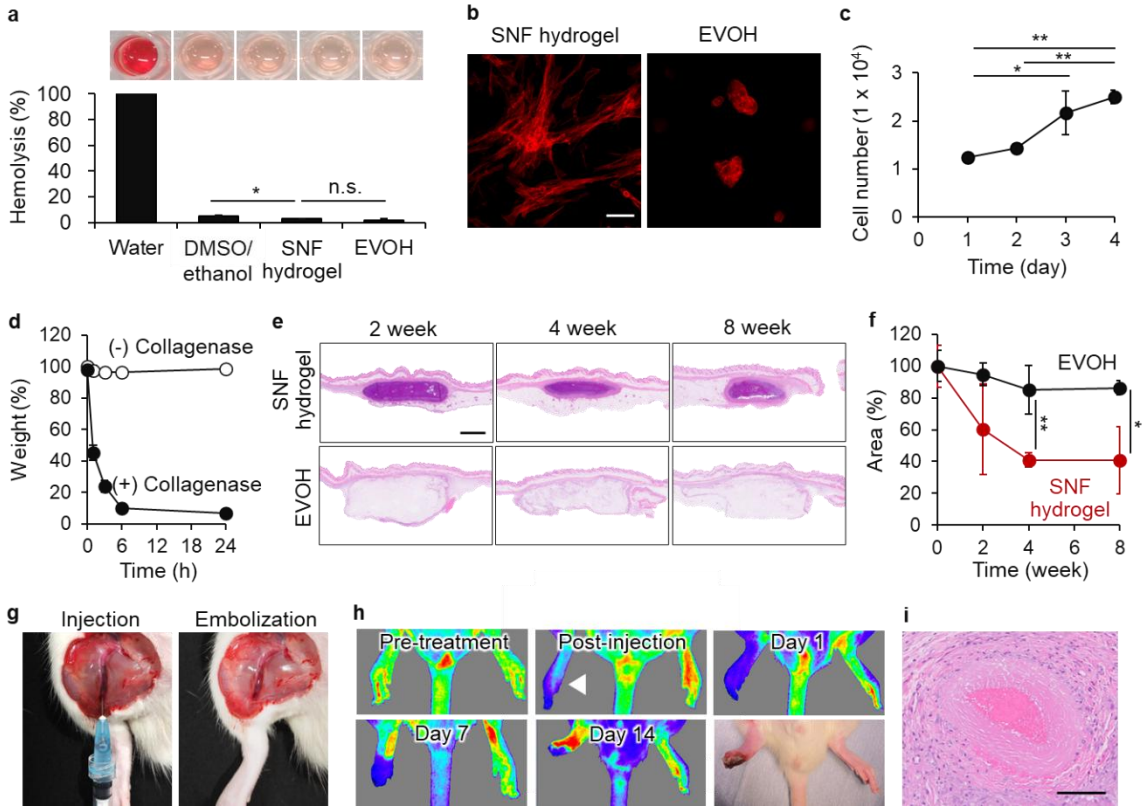

Figure 5. (a) Hemolysis assay of SNF hydrogel and EVOH (n=3). (b) CLSM images of NHDFs seeded onto SNF hydrogels and EVOH. Actin was stained with phalloidin. (c) Proliferation assay of NHDFs on SNF hydrogels (n=3). (d) Degradability test of SNF hydrogels using collagenase (n = 3). (e, f) HE images of SNF hydrogels and EVOH at 2, 4, and 8 weeks after subcutaneous implantation into mice and their quantification of the change of cross-sectional area. (g) Photos of injection of SNF hydrogels into femoral artery of rats. (h) Hindlimb blood flow monitored using a laser Doppler imaging system pre- and post-injection. SNF hydrogels were injected into femoral artery of right legs. (i) HE image of femoral artery at 14 days after the injection. Data are presented as the mean ± s.d. **P* < 0.05, ***P* < 0.01 analyzed by one-way ANOVA with Tukey's multiple comparison *post hoc* test for (a,c) and Student's *t*-test for (f). Scale bars represent 50 μm for (b) and 1 mm for (e).

3.5 Machine learning-driven exploration

Finally, an ALBO pipeline is employed to explore further the composition of the embolic agents (Figure 6a). Based on the initial experimental results (viscosity and blood coagulation of the tGUPy-based embolic agent), several compositions with different parameters (feeding ratio of UPy units, polymer concentration, and solvent composition) were proposed. After performing 3 ALBO cycles, one candidate (tGUPy-8, 3 wt%, 40% ethanol in DMSO) with very low viscosity (7.0 mPa•s) and high blood coagulation (94%) was discovered (Figure 6b). Low-viscosity embolic agents can penetrate deep into the nidus and help treat diseases that require distal penetration.[31, 35] For example, Onyx®-18 shows more distal penetration into the arteriovenous malformation nidus.[36] Therefore, this material informatics approach shows great potential for accelerating the optimisation of embolic agents with high functionality.

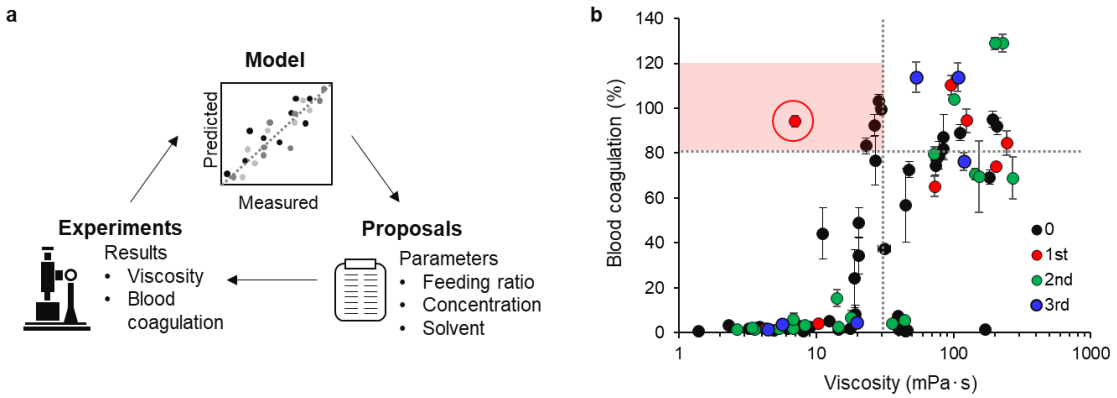

Figure 6. (a) Schematic illustration of machine learning process. (b) Relationship between viscosity and blood coagulation (n=3). The data were overlapped to the result shown in Figure 2e (black filled circle, 0). Machine learning process repeated three times (1st, 2nd, 3rd). Data are presented as the mean ± s.d. for (b).

4. Conclusion

In conclusion, we presented the design of a biodegradable liquid embolic agent that forms nanofiber hydrogels in blood. Chemical modification of gelatin with hydrogen-bonding moieties at high D.S. produced water-insoluble blood-coagulating protein-based embolic agents. Injection of the GUPy solution formed hydrogels with nanofiber network structures, which demonstrated high blood coagulation ability and high injectability. The SNF hydrogels exhibited tissue-adhesive properties to blood vessel walls, whereas weak adhesiveness to catheter tubes was confirmed. In vitro and in vivo experiments showed that SNF hydrogels possess high hemocompatibility, cell adhesion, proliferative properties, and biodegradability. SNF hydrogels demonstrated embolization of rat femoral arteries. Furthermore, the machine-learning-based approach suggested a composition of embolic agents with low viscosity and high coagulation ability. This in-situ-forming nanofiber hydrogel may serve as a biodegradable liquid embolic agent for the treatment of aortic aneurysms, stent grafting, gynecological diseases, and liver cancer in IVR therapy.

Supporting Information

Supporting Information is available from the Wiley Online Library or from the author.

Acknowledgements

We appreciate financial support from the Japan Society for the Promotion of Science (JSPS) KAKENHI (grant nos. 22H03962 and 23H01718), the Uehara Memorial Foundation, and the Inamori Foundation (Inamori Research Grants).

Received: ((will be filled in by the editorial staff))
Revised: ((will be filled in by the editorial staff))
Published online: ((will be filled in by the editorial staff))

References

[1] R. A. Sheth, S. Sabir, S. Krishnamurthy, R. K. Avery, Y. S. Zhang, A. Khademhosseini, R. Oklu, *J Funct Biomater* **2017**, 8, 12.
[2] J. Hu, H. Albadawi, B. W. Chong, A. R. Deipolyi, R. A. Sheth, A. Khademhosseini, R. Oklu, *Adv Mater* **2019**, 31, e1901071.
[3] A. Perez-Lopez, C. Martin-Sabroso, L. Gomez-Lazaro, A. I. Torres-Suarez, J. Aparicio-Blanco, *Acta Biomater* **2022**, 149, 1.

[4] M. Bendszus, R. Klein, R. Burger, M. Warmuth-Metz, E. Hofmann, L. Solymosi, *AJNR Am J Neuroradiol* **2000**, 21, 255.
[5] A. Pal, J. Blanzy, K. J. R. Gomez, M. C. Preul, B. L. Vernon, *Gels* **2023**, 9.
[6] A. J. Molyneux, S. Cekirge, I. Saatci, G. Gál, *AJNR Am J Neuroradiol* **2004**, 25, 39.
[7] Menghui Liu, Yunzhi Wang, Yanlv Chen, Liujun Li, Yang Sun, Yongchao Li, Yajun Yuan, Pan Lu, Wenkai Zhang, Pengfei Pang, Xin Peng, H. Shan, *Adv. Funct. Mater.* **2023**, 33, 2305153.
[8] T. F. X. O'Donnell, S. E. Deery, L. T. Boitano, J. J. Siracuse, M. L. Schermerhorn, S. T. Scali, A. Schanzer, R. T. Lancaster, V. I. Patel, *J Vasc Surg* **2019**, 69, 414.
[9] B. Richling, *Acta Neurochirurgica* **1982**, 64, 109.
[10] W. Taki, Y. Yonekawa, H. Iwata, A. Uno, K. Yamashita, H. Amemiya, *AJNR Am J Neuroradiol* **1990**, 11, 163.
[11] H. S. Cekirge, I. Saatci, M. H. Ozturk, B. Cil, A. Arat, M. Mawad, F. Ergungor, D. Belen, U. Er, S. Turk, M. Bavbek, Z. Sekerci, E. Beskonakli, O. E. Ozcan, T. Ozgen, *Neuroradiology* **2006**, 48, 113.
[12] Y. Matsumaru, A. Hyodo, T. Nose, S. Ito, T. Hirano, S. Ohashi, *J Biomater Sci Polym Ed* **1996**, 7, 795.
[13] H. Yang, K. Lei, F. Zhou, X. Yang, Q. An, W. Zhu, L. Yu, J. Ding, *Mater Sci Eng C Mater Biol Appl* **2019**, 102, 606.
[14] J. Hu, I. Altun, Z. Zhang, H. Albadawi, M. A. Salomao, J. L. Mayer, L. Hemachandra, S. Rehman, R. Oklu, *Adv Mater* **2020**, 32, e2002611.
[15] J. Hu, H. Albadawi, Z. Zhang, M. A. Salomao, S. Gunduz, S. Rehman, L. D'Amone, J. L. Mayer, F. Omenetto, R. Oklu, *Adv Mater* **2022**, 34, e2106865.
[16] Z. Zhang, H. Albadawi, R. J. Fowl, I. Altun, M. A. Salomao, J. Jahanyar, B. W. Chong, J. L. Mayer, R. Oklu, *Adv Mater* **2022**, 34, e2108266.
[17] R. Xie, Y. C. Chen, Y. Zhao, N. Yodsanit, Y. Wang, N. Yamamoto, D. Yamanouchi, S. Gong, *ACS Appl Mater Interfaces* **2021**, 13, 56988.
[18] Z. Jin, H. Fan, T. Osanai, T. Nonoyama, T. Kurokawa, H. Hyodoh, K. Matoba, A. Takeuchi, J. P. Gong, M. Fujimura, *Proc Natl Acad Sci U S A* **2022**, 119, e2206685119.
[19] X. Lu, X. Li, J. Yu, B. Ding, *Acta Biomater* **2022**.
[20] Z. Yang, L. Chen, J. Liu, H. Zhuang, W. Lin, C. Li, X. Zhao, *Adv Mater* **2023**, 35, e2301849.
[21] Bryan B. Hsu, William Conway, Cory M. Tschabrunn, Manav Mehta, Monica B. Perez-Cuevas, Shuguang Zhang, P. T. Hammond, *ACS Nano* **2015**, 9, 9394.
[22] P. Nakielski, F. Pierini, *Acta Biomater* **2019**, 84, 63.
[23] A. Nishiguchi, H. Ichimaru, S. Ito, K. Nagasaka, T. Taguchi, *Acta Biomater* **2022**, 146, 80.
[24] A. Nishiguchi, S. Ito, K. Nagasaka, T. Taguchi, *Biomacromolecules* **2023**, 24, 1545.
[25] A. Nishiguchi, S. Ito, K. Nagasaka, H. Komatsu, K. Uto, T. Taguchi, *Biomaterials* **2024**, 305, 122451.
[26] Brigitte J. B. Folmer, Rint P. Sijbesma, Ron M. Versteegen, Joost A. J. van der Rijt, E. W. Meijer, *Adv Mater* **2000**, 12, 874.
[27] R. Zamani Alavijeh, P. Shokrollahi, J. Barzin, *J. Mater. Chem. B* **2017**, 5, 2302.
[28] A. Nishiguchi, F. Sasaki, H. Maeda, M. Kabayama, A. Ido, T. Taguchi, *Small* **2019**, 15, e1901566.
[29] Christophe Bajan, G. Lambard, *MADGUI: Multi-Application Design Graphical User Interface. GitHub.* *https://github.com/Lambard-ML-Team/MADGUI*.
[30] H. A. Belcher, M. Guthold, N. E. Hudson, *Res Pract Thromb Haemost* **2023**, 7, 100285.
[31] D. F. Vollherbst, R. Otto, T. Do, H. U. Kauczor, M. Bendszus, C. M. Sommer, M. A. Möhlenbruch, *Interventional Neuroradiology* **2018**, 24, 693.

[32] J. Lord, H. Britton, S. G. Spain, A. L. Lewis, *J Mater Chem B* **2020**, 8, 8207.
[33] T. E. Robinson, E. A. B. Hughes, A. Bose, E. A. Cornish, J. Y. Teo, N. M. Eisenstein, L. M. Grover, S. C. Cox, *Adv Healthc Mater* **2020**, 9, e1901521.
[34] C. Senturk, *Cardiovasc Intervent Radiol* **2015**, 38, 1654.
[35] S. K. Natarajan, D. Born, B. Ghodke, G. W. Britz, L. N. Sekhar, *J Neurosurg* **2009**, 111, 105.
[36] H. Jin, Z. Liu, Q. Chang, C. Chen, H. Ge, X. Lv, Y. Li, *Interv. Neuroradiol.* **2017**, 23, 497.

Biodegradable liquid embolic agents are used in interventional radiology. A solution of gelatin modified with hydrogen-bonding moieties can form nanofiber hydrogels in the blood for endovascular embolization. The nanofiber hydrogel system exhibits tissue-adhesive properties to blood vessels, non-adhesive properties to catheter tubes, and biodegradability. This nanofiber hydrogel may serve as a biodegradable liquid embolic agent for interventional radiology applications.

Akihiro Nishiguchi*, Miho Ohta, Debabrata Palai, Shima Ito, Kensaku Mori, Ryotaro Akagi, Christophe Bajan, Guillaume Lambard, Keitaro Sodeyama, and Tetsushi Taguchi*

In-situ forming supramolecular nanofiber hydrogel as a biodegradable liquid embolic agent for post-embolization tissue remodeling

Supporting Information

In-situ forming supramolecular nanofiber hydrogel as a biodegradable liquid embolic agent for post-embolization tissue remodeling

Akihiro Nishiguchi, Miho Ohta, Debabrata Palai, Shima Ito, Kensaku Mori, Ryotaro Akagi, Christophe Bajan, Guillaume Lambard, Keitaro Sodeyama, Tetsushi Taguchi**

Table S1. Synthesis of GUPy derivatives.

	Derivation	Molecular weight	Amino groups in gelatin[a]	Feeding ratio of UPy	Content of UPy	Yield
		(kDa)	(μmol/g)	(molar ratio to amine)	(μmol/g)	(%)
tGUPy-2	tendon	340	269	2	352	85
tGUPy-4	tendon	340	269	4	560	88
tGUPy-10	tendon	340	269	10	524	84
sG(180)UPy-4	skin	180	376	4	515	85
sG(180)UPy-10	skin	180	376	10	1373	91
sG(53)UPy-4	skin	53	343	4	835	83
sG(53)UPy-10	skin	53	343	10	1697	81

[a] The amino groups in as-prepared gelatin and degree of substitution (D.S.) was calculated by determining the residual amino groups using 2,4,6,-trinitrobenzensulfonic acid (TNBS).

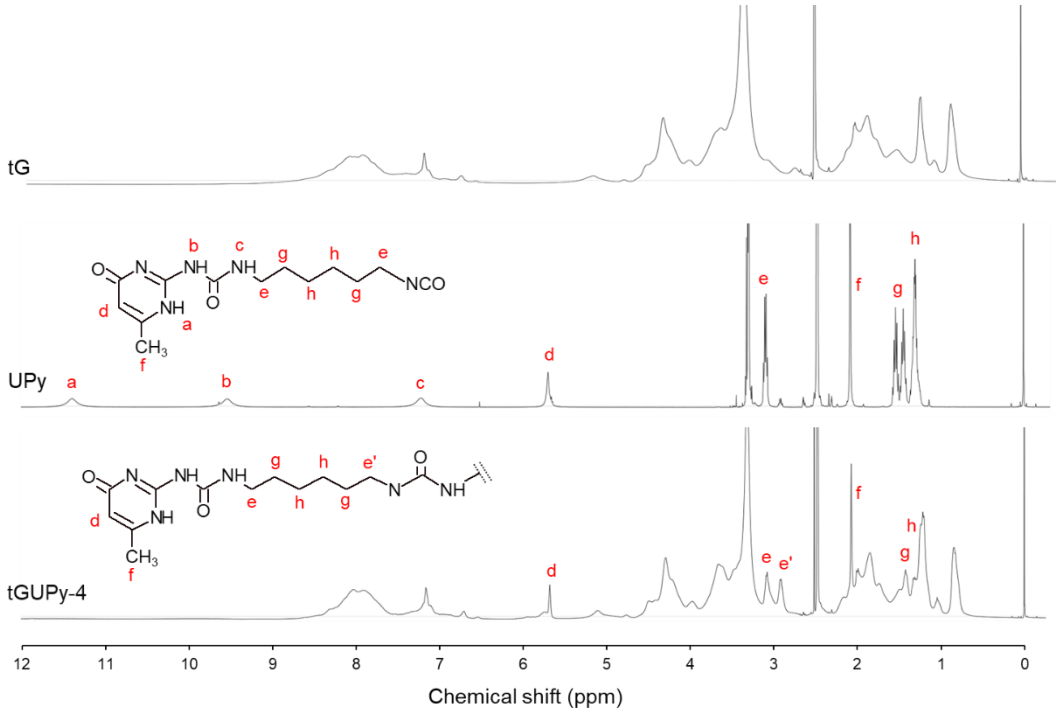

Figure S1. ^{1}H NMR of tG, UPy, and tGUPy-4 (DMSO-d_6, 400 MHz).

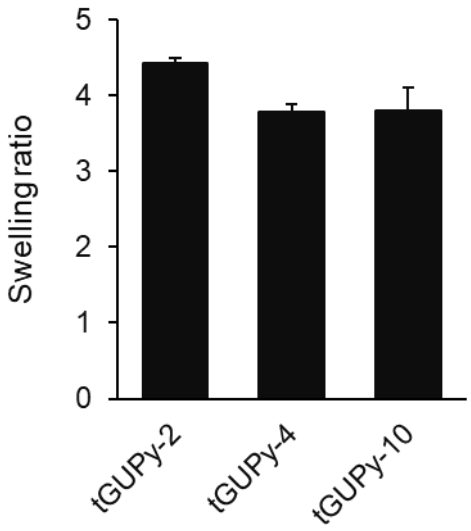

Figure S2. Swelling ratio of SNF hydrogels of tGUPy-2, tGUPy-4, and tGUPy-10 (n=3). Data are presented as the mean ± s.d..

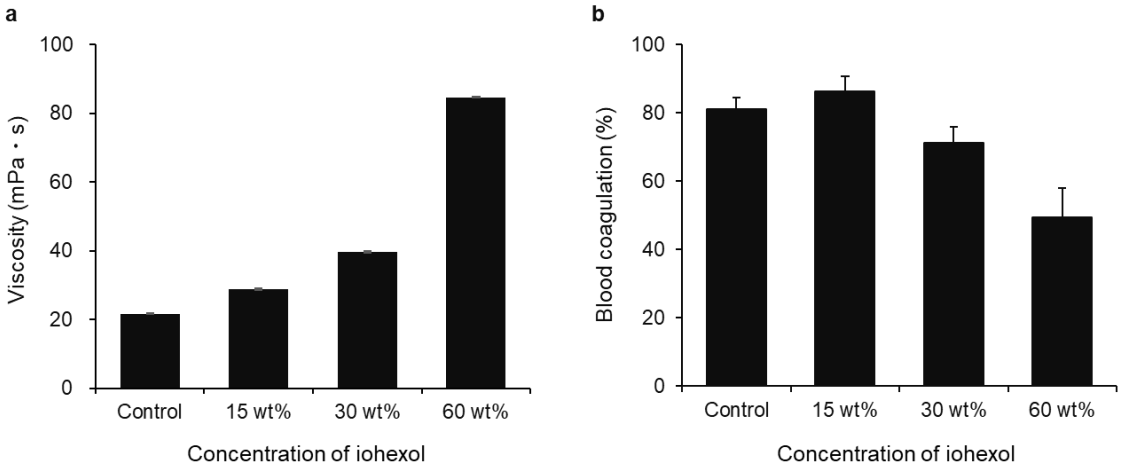

Figure S3. (a,b) Viscosity and blood coagulation of SNF hydrogel with different concentration of iohexol (n=3). Data are presented as the mean ± s.d..

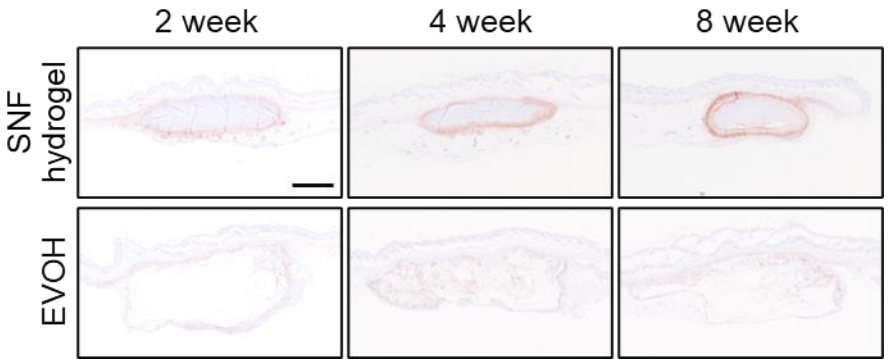

Figure S4. F4/80 stained cross-sectional images of SNF hydrogels and EVOH at 2, 4, and 8 weeks after subcutaneous implantation into mice. Scale bar represents 1 mm.